

Kinematic and Workspace Analysis of the Master Robot in the Sinaflex Robotic Telesurgery System

Mehrnaz Aghanouri, Pejman Kheradmand, Milad Mousavi, Hamid Moradi and Alireza Mirbagheri

Abstract— Robotic telesurgery systems, including master and slave robots, have emerged in recent years to provide benefits for both surgeons and patients. Surgeons use the master manipulator to navigate the slave robot. The Sinaflex telesurgery system introduced recently by Sina Robotics and Medical Innovators Co., Ltd. consists of two main subsystems: master robotic surgery console and slave surgery robots. As the surgeon use the master robot's handles to control the slave surgery robots, it is important for the master robot to provide the ergonomic postures for the surgeon and also providing a large enough workspace and good manipulability for the surgeon to control it. So in this paper, workspace, manipulability and isotropy of each handle at the master robot of the Sinaflex telesurgery system are analyzed. To this end, the kinematic of the master manipulator is derived, and its Jacobian is calculated. Using the simulation environment, the workspace of the master handle is obtained and drawn. The manipulability of the robot for each points of the workspace is computed. According to the results attained from the simulation study, the most manipulability values lie between 0.1 and 0.9 where it is greater than 0.44 for more than 50% of the whole workspace points of the end effector, which is as large as 574×484×560 mm.

I. INTRODUCTION

Telesurgery has gained attention recently as one of the important surgery techniques because of its advantages for both the patients and surgeons over the laparoscopic and conventional surgery. Two main subsystems of the robotic surgery systems are the master and the slave manipulators. Surgeons use the master part to navigate and control the slave manipulator, which does the surgery on the patient. To provide the dexterity and an ergonomic state, the workspace of the master manipulator should be big enough and dexterous [1, 2].

M. Aghanouri is with the Department of Medical Physics and Biomedical Engineering, School of Medicine, Tehran University of Medical Sciences, Tehran, Iran (e-mail: m-aghanouri@razi.tums.ac.ir)

P. Kheradmand and M. Mousavi are with the Research Center for Biomedical Technologies and Robotics (RCBTR), Advanced Medical Technologies and Equipment Institute (AMTEI), Tehran University of Medical Sciences (TUMS), Tehran, Iran.

H. Moradi is with the Department of Medical Physics and Biomedical Engineering, School of Medicine, Tehran University of Medical Sciences, Tehran, Iran.

A. Mirbagheri, is with the Department of Medical Physics and Biomedical Engineering, School of Medicine and joint affiliated with Research Center for Biomedical Technologies and Robotics (RCBTR), Advanced Medical Technologies and Equipment Institute (AMTEI), Tehran University of Medical Sciences (TUMS), Tehran, Iran. (phone: 0098-21-64053245; fax: 0098-21-66482654; e-mail: a-mirbagheri@tums.ac.ir).

Various master robots have been designed with the aim of the telesurgery. The most famous surgical robotic system is daVinci surgical system (Intuitive Surgical Inc., Sunnyvale, California, United States) whose master manipulator is an 8-DoF serial robot employing cable driven and gear transmission mechanisms [3]. The master part of the Senhance surgical system (Asensus Surgical Inc., Miami, Florida, United States) utilizes haptic handlebars [4]. An 8-DOF serial manipulator is proposed in [5] including arm, wrist and clamp mechanisms. the position is adjusted using the first three joints, and the orientation and the clamp motion are determined by the rest of the joints. A 7-DoF serial manipulator including gripping DoF is proposed by Lee et. al [6], where two revolute and one prismatic joints are used to control the RCM position and a gimbal mechanism provides 3 rotational DoFs. In [7, 8] (a modified version of the 5-DOF Haptic Wand [9]), a parallel mechanism, is proposed. This mechanism comprises a dual-pantograph arrangement, which provide 5 DoFs including 3 translation and 2 rotation DoFs, the cable-driven differential transmissions and DC motors enabling yaw angle and grasping. Due to their accuracy in the position and force-feedback as the input and output, haptic interfaces are used as the master manipulator in robotic surgical systems like Raven-II [10, 11] which uses a 6-DoF PHANTOM haptic interface, and the DLR Miro-SurgeHaptic which employs a 7-DoF Omega.7 haptic interface including grasping DoF [12, 13]. These haptic devices employ either the serial mechanisms (like PHANTOM series haptic interface) or the parallel mechanisms (like Omega.7 and Sigma.7). Each of these types of the mechanisms has the advantages and disadvantages. The serial mechanisms provide a large workspace, dexterous operation, and relatively easy solution for forward and inverse kinematic equations, while they have relatively the small mechanical stiffness, high inertia, and a large end effector position error [14]. Contrary to the serial mechanisms, the parallel structures offer the large stiffness, small inertia, small error in end effector position, and fast dynamic response. However, their workspace is relatively small, and the forward and inverse kinematic equations have complicated solutions. To overcome these limitations, the hybrid mechanisms, a combination of serial and parallel structures, are introduced [14]. However, providing the rotational force feedback is not straightforward in such mechanisms. A hybrid master manipulator is proposed by Li, et. al [15], in which the parallel part is responsible for the position control and the redundant serial part is used for the orientation control. A 9-DoF manipulator is presented in [1], in which a parallelogram and an active compensation mechanisms are used to separate translational and rotational DoFs.

Sina_{flex} robotic telesurgery system [16] (Sina Robotics and Medical Innovators Co., Ltd., Tehran, Iran) is a new telesurgery platform which has been developed to accomplish the remote surgery aims. As the other telesurgery robotic systems, Sina_{flex} has the master console and the slave part. Despite the other telesurgery systems, this system provides adjustable master console, from sitting to standing, to make the convenient states for the surgeons. Besides, it has a three DoFs force feedback mechanism to help the surgeon feels the kinesthetic forces in contact with the environment. The master robotic console has 19 DoFs comprising 7 DoFs for each handle itself designed by employing hybrid mechanisms. The slave robotic subsystem has 35 DoFs comprising 7 DoFs for each surgical robot. The technical information of each part is discussed in [16]. As it is mentioned before, the workspace and dexterity analysis is crucial for the master manipulator to prove it is ergonomic and functional.

This study, to the best of the authors' knowledge, is the first study in which the master robot of the Sina_{flex} robotic telesurgery system [16] is analyzed. The main purpose in this study is the workspace and manipulability analysis of the master manipulator in Sina_{flex} robotic telesurgery system. To this end, first, the kinematic equations and the Jacobian matrix of the master part are derived. Then, the workspace is obtained and finally, the manipulability of the robot is investigated.

This paper consists of 7 sections. The master manipulator is introduced in section 2. The kinematic model is derived in section 3. The workspace and the manipulability are analyzed in sections 4 and 5, respectively. The simulation results and discussion are explained in section 6, and finally the conclusion and future work are drawn in section 7.

II. SYSTEM OVERVIEW

The master robot of the Sina_{flex} telesurgery system (Fig. 1) consists of two handles each of which has 7 DoFs. Each handle consists of two parts: a semi-parallelgram mechanism and a serial spherical robot (Fig. 2). The Cartesian position and the orientation of the handle are specified by the first and second parts, respectively. The spherical part is rotated around the RCM which is located at the intersection of the spherical part joints axes and the extension of the last link of the semi-parallelgram mechanism. To provide a 3 DoF haptic force feedback, three motors are mounted on the 3 active joints of the semi-parallelgram part. Three encoders are used at the next three joints to read the angles to provide the orientation information.

The kinematic model of each handle is derived for the parallel and series mechanisms separately and then the equations are merged. The details are explained in the following.

A. Kinematic Model of the Semi-Parallelgram Part

The reference frame is defined at last joint of the semi-parallelgram part, which is called the end effector of the semi-parallelgram mechanism (*ee1*). As the first step to analyze the kinematic of this part, local frames are defined



Figure 1. The SINA_{flex} robotic telesurgery system, left: the slave robot, right: the master robot [17].

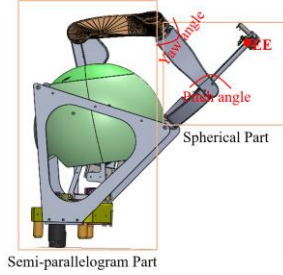


Figure 2. The handle of the master manipulator.

for each active joint. The rotation matrix between the *ee1* frame and the reference frame is calculated as:

$$\begin{cases} {}^0R_{ee1} = {}^0R_1 {}^1R_{ee1} \\ {}^0R_1 = Rot(z, \theta_1) \\ {}^1R_{ee1} = Rot(x, -\theta_3) \end{cases} \Rightarrow {}^0R_{ee1} = \begin{bmatrix} \cos(\theta_1) & -\cos(\theta_3)\sin(\theta_1) & -\sin(\theta_3)\sin(\theta_1) \\ \sin(\theta_1) & \cos(\theta_3)\cos(\theta_1) & \sin(\theta_3)\cos(\theta_1) \\ 0 & -\sin(\theta_3) & \cos(\theta_3) \end{bmatrix} \quad (1)$$

B. Kinematic Model of the Spherical Part

Since the spherical part is a serial mechanism, the conventional Denavit-Hartenberg (D-H) method is employed to derive the kinematic equations for this part. Table I. shows the D-H parameters. The *ee* frame is considered at the RCM. The rotation matrix between the RCM and the considered reference frame for the gimbal mechanism (0g) is calculated as:

$${}^0gR_{ee} = {}^0gR_1 {}^1R_2 {}^2R_{ee} = \begin{bmatrix} r_{11} & r_{12} & r_{13} \\ r_{21} & r_{22} & r_{23} \\ r_{31} & r_{32} & r_{33} \end{bmatrix} \quad (2)$$

$$\begin{aligned} r_{11} &= C_{yaw}S_{roll} + S_{yaw}S_{pitch}C_{roll}, r_{12} = C_{yaw}C_{roll} - S_{yaw}S_{pitch}S_{roll}, r_{13} = -S_{yaw}C_{pitch}, \\ r_{21} &= S_{yaw}S_{roll} + C_{yaw}S_{pitch}C_{roll}, r_{22} = S_{yaw}C_{roll} + C_{yaw}S_{pitch}S_{roll}, r_{23} = C_{yaw}C_{pitch}, \\ r_{31} &= C_{pitch}C_{roll}, r_{32} = -C_{pitch}S_{roll}, r_{33} = S_{pitch} \end{aligned}$$

$${}^0gR_1 = Rot\left(z, \theta_{pitch} + \frac{\pi}{2}\right) Rot(x, \alpha_1)$$

$${}^1R_2 = Rot\left(z, \theta_{yaw} + \frac{\pi}{2}\right) Rot(x, \alpha_2)$$

$${}^2R_{ee} = Rot(z, \theta_{roll})$$

in which, $C \equiv \cos$ and $S \equiv \sin$.

TABLE I. THE DENAVIT-HARTENBERG PRAMETERS.

i	The Denavit-Hartenberg Parameters			
	d_i	θ_i	a_{i-1}	α_{i-1}
1	0	$\theta_{yaw} - \frac{\pi}{2}$	0	0
2	0	$\theta_{pitch} - \frac{\pi}{2}$	0	$\frac{\pi}{2}$
3	0	θ_3	0	$\frac{\pi}{2}$

C. Kinematic of the Whole Mechanism

As the first step, the rotation matrix between frame 0_g and the frame $ee1$ (${}^{ee1}R_{0_g}$) is derived for the manipulator using the kinematic model of the robot as:

$${}^{ee1}R_{0_g} = {}^{ee1}R_s {}^sR_{0_g} \quad (3)$$

Then, using (1), (2) and (3), ${}^0R_{ee}$ is calculated as:

$${}^0R_{ee} = {}^0R_{ee1} {}^{ee1}R_{0_g} {}^{0_g}R_{ee} \quad (4)$$

III. THE WORKSPACE ANALYSIS

To show how much dexterous the master robot is, the workspace of the end effector (the point where the operator moves) is obtained. To this end, the position of the end effector (${}^0P_{EE}$) is calculated for different angles of the joints. Since the end effector moves on a sphere with the center of RCM, the end effector position can be derived as:

$${}^0P_{EE} = {}^0P_{RCM} + {}^0R_{ee} \begin{bmatrix} 0 \\ 0 \\ r_{EE} \end{bmatrix} \quad (5)$$

where ${}^0P_{RCM} = [x_{RCM} \ y_{RCM} \ z_{RCM}]^T$ and r_{EE} is the distance between the RCM and the end effector.

To evaluate the dexterity of the master manipulator, different indices are introduced in the literature such as the condition number (isotropy), the manipulability, and the minimum singular value [2, 18]. In this paper, the condition number (isotropy) and the manipulability are calculated for the $Sina_{flex}$ master manipulator as:

$$\begin{aligned} \text{Condition number: } I_1 &= \frac{\sigma_{max}}{\sigma_{min}} \\ \text{Manipulability: } I_2 &= 1/I_1 \end{aligned} \quad (6)$$

where, σ_{min} and σ_{max} are the smallest and largest singular values of the Jacobian matrix (J), respectively. The condition number lies between 1 and ∞ , where value 1 shows the isotropic configuration. To calculate the Jacobian, the method proposed in [19] is employed. This process is described in the following section.

To investigate the manipulability over the whole workspace, the global conditioning index (GCI) is used. Since the manipulability is calculated discretely (the process is explained in section V), the discreet GCI is calculated as:

$$\widetilde{GCI} = \sum_{i=1}^N I_2/N \quad (7)$$

in which, N indicates the number of the workspace points where the manipulability is calculated.

A. The Jacobian Calculation

In this method [19], two parts of the Jacobian (8), J_v and J_ω , which are related to linear and angular velocity, are calculated independently. As the first step, the matrix L , is defined as (9).

$$J = \begin{bmatrix} [J_v]_{3 \times 3} & 0_{3 \times 3} \\ & [J_\omega]_{3 \times 6} \end{bmatrix} \quad (8)$$

$$L = [\partial {}^0H_{ee}/\partial \theta_1 \ \dots \ \partial {}^0H_{ee}/\partial \theta_6] \quad (9)$$

where, ${}^0H_{ee} = \begin{bmatrix} {}^0R_{ee} & {}^0P_{RCM} \\ 0_{1 \times 3} & 1 \end{bmatrix}$.

Then, J_v is calculated as follows:

$$J_v = Lp, p = 1_{6 \times 6} \otimes \begin{bmatrix} 0 \\ 0 \\ 0 \\ 1 \end{bmatrix} \quad (10)$$

To derive J_ω , the inverse of ${}^0H_{ee}$ is calculated. By defining $J_{p\omega} = L_i {}^0H_{ee}^{-1}$, in which i is the i^{th} 4×4 block of matrix L , J_ω is calculated as follows:

$$J_\omega = \begin{bmatrix} (L_i {}^0H_{ee}^{-1})_{(3,2)} & (L_i {}^0H_{ee}^{-1})_{(1,3)} & (L_i {}^0H_{ee}^{-1})_{(2,1)} \end{bmatrix}^T \quad (11)$$

IV. SIMULATION RESULTS

For the simulation analysis, MALAB 2019b (MathWorks, Massachusetts, United States) is used. To derive the workspace, the roll axis is not considered due to the symmetry. The position of the end effector (EE) is calculated for different values of $(\theta_1, \theta_2, \theta_3, \theta_{yaw}, \theta_{pitch})$, where no collision exits. Fig. 3 shows the obtained workspace.

To represent the manipulability, using (8) to (11), the Jacobian is calculated for each set of angles $(\theta_1, \theta_2, \theta_3, \theta_{yaw}, \theta_{pitch})$ in the workspace. Then by exploiting the singular value decomposition method, the singular values containing the minimum and maximum values are obtained for each values of the Jacobian. Finally, the manipulability is calculated using (6). Fig. 4 shows the manipulability values in the Cartesian space. As it can be seen, the order of the manipulability values is 10^{-1} . The closer the manipulability values to 1, the more isotropic and dexterous the robot is. The iso-manipulability points of the workspace in X-Y, Y-Z, and X-Z planes are plotted in Fig. 5. The calculated value of \widetilde{GCI} for 508200 points in the workspace using (7) is 0.44.

V. CONCLUSION

In this paper, the kinematic of the novel master robot of the $Sina_{flex}$ robotic telesurgery system is obtained. This robot comprises two parts including a semi-parallelogram mechanism and a serial spherical mechanism. The kinematic of the whole mechanism is represented by merging the obtained kinematics of each mechanism. Using the homogenous matrix, the Jacobian matrix is derived and the manipulability of the robot is analyzed. The simulation

results show that the manipulability is between 0.1 and 0.9, and the \overline{GCI} value is 0.44 for the whole large workspace which is 574×484×560 mm. These results prove the dexterity and functionality of the master robot during the telesurgery operations. As the future work, the manipulability of the master robot will be investigated experimentally in the operable space by defining some tasks similar to the surgical tasks like suturing.

Figure 3. The workspace of the handle for different values of the joints'

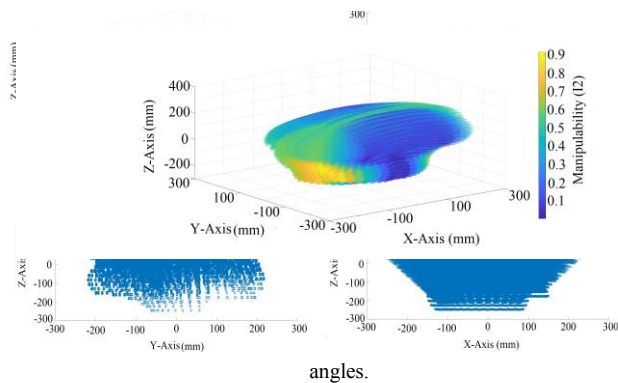


Figure 4. The manipulability values for the different points of the workspace.

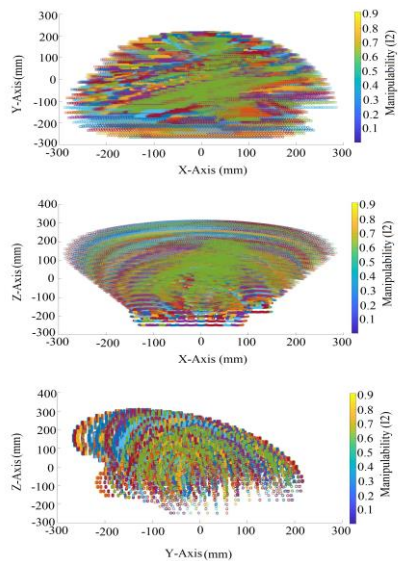


Figure 5. The iso-manipulability points of the workspace in different planes.

In this study, neither human subjects nor animals are involved.

REFERENCES

[1] Y. Liang, L. Sun, Z. Du, Z. Yan, and W. Wang, "Mechanism design and optimization of a haptic master manipulator for laparoscopic surgical robots," *J IEEE Access*, vol. 7, pp. 147808-147824, 2019.

[2] D. Zhang, J. Liu, A. Gao, and G.-Z. Yang, "An ergonomic shared workspace analysis framework for the optimal placement of a compact master control console," *J IEEE Robotics Automation Letters*, vol. 5, no. 2, pp. 2995-3002, 2020.

[3] C. Freschi, V. Ferrari, F. Melfi, M. Ferrari, F. Mosca, and A. Cuschieri, "Technical review of the da Vinci surgical telemanipulator," *J The International Journal of Medical Robotics Computer Assisted Surgery*, vol. 9, no. 4, pp. 396-406, 2013.

[4] D. Stephan, H. Sälzer, and F. Willeke, "First experiences with the new Senhance® telerobotic system in visceral surgery," *J Visceral medicine*, vol. 34, no. 1, pp. 31-36, 2018.

[5] X. Chen, X. Xin, B. Zhao, Y. He, Y. Hu, and S. Liu, "Design and analysis of a haptic master manipulator for minimally invasive surgery," in *2017 IEEE International Conference on Information and Automation (ICIA)*, 2017, pp. 260-265: IEEE.

[6] H. Lee, B. Cheon, M. Hwang, D. Kang, D. S. J. T. I. J. o. M. R. Kwon, and C. A. Surgery, "A master manipulator with a remote-center-of-motion kinematic structure for a minimally invasive robotic surgical system," vol. 14, no. 1, p. e1865, 2018.

[7] S. Perreault, A. Talasz, A. L. Trejos, C. D. Ward, R. V. Patel, and B. Kiaii, "A 7-DOF haptics-enabled teleoperated robotic system: Kinematic modeling and experimental verification," in *2010 3rd IEEE RAS & EMBS International Conference on Biomedical Robotics and Biomechanics*, 2010, pp. 906-911: IEEE.

[8] H. Bassan, A. Talasz, and R. V. Patel, "Design and characterization of a 7-DOF haptic interface for a minimally invasive surgery test-bed," in *2009 IEEE/RSJ International Conference on Intelligent Robots and Systems*, 2009, pp. 4098-4103: IEEE.

[9] (2021, 3/25) Available: https://docs.quanser.com/quarc/documentation/quanser_5dof_wa nd_blocks.html

[10] A. Bhardwaj, A. Jain, and V. Agarwal, "Preoperative planning simulator with haptic feedback for Raven-II surgical robotics platform," in *2016 3rd International Conference on Computing for Sustainable Global Development (INDIACom)*, 2016, pp. 2443-2448: IEEE.

[11] B. Hannaford *et al.*, "Raven-II: an open platform for surgical robotics research," *J IEEE Transactions on Biomedical Engineering*, vol. 60, no. 4, pp. 954-959, 2012.

[12] R. Konietzschke *et al.*, "The DLR MiroSurge-A robotic system for surgery," in *2009 IEEE International Conference on Robotics and Automation*, 2009, pp. 1589-1590: IEEE.

[13] U. Hagn *et al.*, "DLR MiroSurge: a versatile system for research in endoscopic telesurgery," *J International journal of computer assisted radiology surgery*, vol. 5, no. 2, pp. 183-193, 2010.

[14] W. Dangxiao, G. Yuan, L. Shiyi, Y. Zhang, X. Weiliang, and X. Jing, "Haptic display for virtual reality: progress and challenges," *J Virtual Reality Intelligent Hardware*, vol. 1, no. 2, pp. 136-162, 2019.

[15] Y. Li, Z. Yan, H. Wang, Z. Du, and Y. Zhang, "Design and optimization of a haptic manipulator using series-parallel mechanism," in *2012 IEEE International Conference on Mechatronics and Automation*, 2012, pp. 2140-2145: IEEE.

[16] M. H. Abedin-Nasab, *Handbook of robotic and image-guided surgery*. Elsevier, 2019.

[17] (2021, 3/25). Available: <https://sinamed.ir/>

[18] J.-P. Merlet, "Jacobian, manipulability, condition number, and accuracy of parallel robots," 2006.

[19] P. Chembrammel and T. Kesavadas, "A new implementation for online calculation of manipulator Jacobian," *J PloS one*, vol. 14, no. 2, p. e0212018, 2019.